Methanol Reactions over Oxygen-Modified Re Surfaces: Influence of Surface Structure and Oxidation†

Ally S. Y. Chan,[#] Wenhua Chen,[#] Hao Wang,[#] John E. Rowe,[‡] and Theodore E. Madey*[,#]

Department of Physics & Astronomy and Laboratory for Surface Modification, Rutgers, The State University of New Jersey, Piscataway New Jersey 08854-8019, and Department of Chemistry, The University of North Carolina, Chapel Hill, North Carolina 27599-3290

Received: February 26, 2004; In Final Form: May 5, 2004

The reactions of methanol over planar and faceted oxygen-covered Re(12$\bar{3}$1), and over a thin-film oxide on Re(12$\bar{3}$1), are studied using temperature-programmed desorption (TPD), high-resolution X-ray photoelectron spectroscopy (HRXPS), and low-energy electron diffraction (LEED). These surfaces are potential model catalysts for the selective oxidation of methanol to methylal [dimethoxymethane, $CH_2(CH_3O)_2$]. Re(12$\bar{3}$1) is chosen because it is a morphologically unstable substrate that develops nanometer scale facets when precovered with oxygen and annealed, thus providing a suitable surface to investigate structure−reactivity relationships in methanol decomposition. Reaction pathways for methanol over the O-covered planar and faceted surfaces are qualitatively similar, proceeding through competing pathways of dehydrogenation to CH_2O and CO and nonselective decomposition to yield H_2 and CO that is formed by recombination of $C_{(ads)}$ with surface-bound oxygen. The selectivity toward methanol dehydrogenation products is not affected by morphological differences between the planar and faceted surfaces. However, the activity of the O-modified surfaces decreases progressively in the following order: planar O/Re > faceted O/Re > thin-film oxide/Re, with the thin-film oxide relatively inactive toward methanol reaction. The differences in activity may be attributed to changes in local geometric structure, the oxidation state, and the local order of Re−O species formed on the O-modified Re surfaces. We discuss these results in the context of the elementary steps in the catalytic oxidation of methanol to methylal.

1. Introduction

The chemistry of methanol (CH_3OH) on metal and oxide surfaces is widely studied due to its importance to the chemical industry[1] and its potential as an alternative fuel source.[2] Of particular interest is the selective catalytic oxidation of CH_3OH to products that serve as primary reagents for organic synthesis, for example, formaldehye (CH_2O) and methyl formate ($HC{=}OOCH_3$). Methanol oxidation to formaldehyde is achieved industrially over silver-, molybdena-, and vanadia-based catalysts,[1] while binary metal oxides such as molybdenum−tin oxides[3] and vanadium−titanium oxides[4] are useful for methanol conversion to methyl formate.

Recently, it has been shown that pure and supported Re oxides exhibit high performance for selective methanol oxidation to methylal (dimethoxymethane)[5,6] viz.

$$3CH_3OH + {}^1/_2O_2 \rightarrow CH_2(OCH_3)_2 + 2H_2O$$

A mechanism has been proposed for methylal synthesis, whereby the first step is thought to be the formation of methoxy (CH_3O) species.[5] Dehydrogenation of methoxy subsequently produces formaldehyde, which reacts with specific lattice oxygen in the ReO_x catalyst to form dioxymethylene $(H_2COO)^{2-}$. Oxidative coupling of dioxymethylene with neighboring methoxy and/or methanol is then proposed to yield methylal.[7] Since the elementary step in methylal synthesis is proposed to be the production of formaldehyde via a methoxy intermediate, we aim to investigate evidence for this pathway by reacting methanol over well-defined oxygen-modified Re single-crystal surfaces as model catalysts. Specifically, we are interested in determining if the introduction of nanometer scale features in the model oxygen-modified Re substrate will affect the selectivity of methanol toward partial oxidation products. To this end, we have chosen the Re(12$\bar{3}$1) substrate: this surface retains its planar state when precovered with oxygen at room temperature but converts to a faceted morphology comprising nanoscale ridged facets of (11$\bar{2}$1) and (01$\bar{1}$0) planes when the oxygen-precovered surface is annealed.[8] By employing different preparation methods to achieve the desired geometrical structure for the O-modified Re surfaces, we are able to test for structural effects in methanol reaction pathways. Notably, structural sensitivity in methanol decomposition has previously been observed on Pt surfaces, where C−O bond scission to yield water and adsorbed CH_x species occurs on the Pt(110)-(1 × 1) surface, while methoxy formation dominates on the reconstructed Pt(110)-(2 × 1) surface.[9]

Despite numerous studies concerning methanol chemistry over pure and oxidized metal surfaces, fundamental studies of CH_3OH reactions over well-defined Re surfaces have received relatively sparse attention. On polycrystalline Re comprising mainly (0001)-oriented grains, methanol undergoes complete dehydrogenation to evolve H_2 and CO as the only desorbing products.[10] When methanol is reacted with this same surface that has been precovered with a Pd monolayer and subjected to a high-temperature oxygen treatment, marked differences in methanol reaction pathways are observed—partial oxidation to produce CH_2O and H_2O dominates over complete dehydroge-

† Part of the special issue "Gerhard Ertl Festschrift".
[#] Rutgers University.
[‡] University o2f North Carolina.

10.1021/jp040168x CCC: $27.50
Published on Web 06/29/2004

nation.[10] These changes in reactivity are attributed entirely to the presence of oxygen adsorbed on Pd clusters formed during the oxidation process, and the supporting oxidized Re substrate is reported to be inert toward methanol.

In the present work, we have characterized the different Re−O species formed on O-modified planar and faceted Re surfaces and on a thin-film oxide on Re(12$\bar{3}$1). On the planar and faceted surfaces, we find that methanol reacts via competing pathways of dehydrogenation to CH_2O and CO and nonselective decomposition to yield H_2 and CO formed by recombinative desorption. In contrast, the thin-film oxide exhibits no activity toward methanol reaction due to the high concentration of low oxidation state oxides (ReO, Re_2O_3) on this surface. Striking differences in methanol reactivity are exhibited between the planar and faceted surfaces, which may be ascribed to changes in both the local geometrical structure and the order of oxygen species on these surfaces. Significantly, the fact that formaldehyde is produced from our O-modified Re surfaces suggests that these surfaces may be tailored to stabilize surface-bound $CH_2O_{(ads)}$ and/or dioxymethylene intermediates, thereby providing working catalyst models to investigate the mechanisms for methylal synthesis from methanol.

2. Experimental Section

All experiments are performed in two ultrahigh vacuum chambers with base pressures of $\sim 1 \times 10^{-10}$ Torr, which have been described elsewhere.[11,12] High-resolution X-ray photoelectron spectroscopy (HRXPS) experiments are conducted at the National Synchrotron Light Source on the beamline U4A endstation,[11] which houses a VSW 100 mm hemispherical analyzer operating at a pass energy of 2 eV. The photon energy used is 90 eV, and the total instrumental resolution is approximately 150 meV. The spectra are normalized to account for the gradually decaying photon flux, which is continuously monitored. All spectra shown here are collected at normal emission, with the incident photon at 45° to the sample surface. Re 4f binding energies have been calibrated with respect to the Fermi level. Analysis of Re 4f spectra is performed using a nonlinear least-squares fit to a Doniach−Sunjic function[13] that is convoluted with a Gaussian to account for instrumental, phonon, and inhomogeneous broadening. The Doniach−Sunjic function, commonly used to describe line shapes of metallic core levels, has two parameters: the Lorentzian width Γ (lifetime broadening of the core hole) and the singularity index α (asymmetry due to final state screening effects in metals). The spectral background includes a correction for overlapping $5p_{1/2}$ contribution into the low binding energy tail of the Re $4f_{7/2}$ peak.[14]

Temperature-programmed desorption (TPD) experiments are conducted at Rutgers in a chamber, previously described,[12] that is equipped with low-energy electron diffraction (LEED) optics, a cylindrical mirror analyzer with concentric electron gun for Auger electron spectroscopy (AES), and a quadrupole mass spectrometer (QMS) capable of sampling up to 10 masses in a single temperature-programmed desorption sweep. Resistive heating to 950 K ($dT/dt \sim 5$ K s^{-1}) is used in all TPD experiments, and product evolution is measured with the QMS in line-of-sight to the crystal. Sample temperature is measured using a W(5%)Re−W(26%)Re thermocouple spot-welded to the back of the crystal.

The Re(12$\bar{3}$1) crystal (10 mm in diameter) is initially cleaned by oxidation at 1000 K in 5×10^{-9} Torr of oxygen, followed by repeated flashing to 2300 K. A sharp (1×1) LEED pattern for planar Re(12$\bar{3}$1)is obtained, and surface cleanliness is verified by AES or XPS. After this initial procedure, the Re sample can be cleaned by high-temperature flashes without recourse to an oxidation treatment. The oxygen-covered *planar* surface is formed by background dosing of 5×10^{-8} Torr of O_2 for 1 min with the crystal at room temperature. The oxygen-covered *faceted* surface is obtained by annealing the O-precovered surface in vacuo to 900 K for 2 min. LEED analysis of the annealed surface indicates that the surface has restructured from a planar configuration to a surface comprising ridged nanoscale facets.[8] This faceted surface remains covered with oxygen, as confirmed by AES and HRXPS.

Oxygen (O_2, 99.99%) and isotopically labeled oxygen ($^{18}O_2$, 95−98%) are used without further purification. Anhydrous methanol, CH_3OH (99.998% purity), is subjected to several freeze−pump−thaw cycles prior to use, and its purity verified by mass spectrometry. Methanol is background-dosed at pressures between 1 and 2×10^{-8} Torr onto the Re sample at room temperature. All methanol exposures shown are in Langmuirs ($1\ L = 10^{-6}$ Torr·s $= 133 \times 10^{-6}$ Pa·s) and are uncorrected for ion gauge sensitivity.

3. Results

3.1. Characterization of Oxygen-Covered Planar and Faceted Re(12$\bar{3}$1). The LEED patterns of clean planar, O-covered planar, and O-induced faceted Re(12$\bar{3}$1) are shown in Figure 1. The atomically rough clean Re(12$\bar{3}$1) surface comprises six layers of exposed surface atoms (Figure 2), which retains the planar (1×1) LEED structure under ultrahigh vacuum conditions (Figure 1a). Upon adsorption of oxygen at 300 K, ranging from 0.5 to 50 L of O_2 exposure, no additional LEED spots are observed when compared with the LEED pattern of the clean surface taken at the same incident electron beam energy (Figure 1a,b). However, an increase in diffuse background intensity is noted, which suggests that the as-dosed oxygen overlayer is disordered. Increasing the incident electron beam energy for the oxygen-dosed surface leads to the motion and convergence of the diffracted beams to the center (0,0) position. All these observations indicate that the chemisorbed oxygen overlayer does not form a long-range periodic structure on Re(12$\bar{3}$1) and that the O-covered Re surface remains planar at 300 K.

Annealing the O-precovered surface to temperatures above 700 K leads to drastic restructuring of the surface to form nanosized facets with a ridged "hill-and-valley" morphology. Additional LEED spots are observed for the annealed surface, compared with the O-covered planar surface at 300 K (Figure 1b,c). When the energy of the incident beam is increased, the diffracted beams move and converge to fixed positions that correspond to the specularly reflected beams of (11$\bar{2}$1) and (01$\bar{1}$0) facets. These facet orientations are confirmed by kinematic simulations of the LEED patterns observed for O-induced faceted Re formed by annealing to 900 K. A detailed LEED study on the faceting of Re(12$\bar{3}$1) induced by oxygen will be published elsewhere.[8]

The minimum O_2 dose at 300 K that is required to induce faceting of the Re substrate upon annealing is $\sim$0.5 L; using this O_2 exposure, partial faceting of the substrate is observed, based on the coexistence of LEED features attributed to both the planar and faceted surfaces.[8] At higher O_2 exposures $\geq$ 1 L, the annealed substrate is fully faceted, exhibiting LEED structures that are due only to the faceted surface. The same faceted morphology is formed upon predosing Re(12$\bar{3}$1) with O_2 exposures ranging from 1 to 50 L and annealing to 900 K to induce faceting. In HRXPS characterization of the O-covered planar and faceted surfaces described below, and for studies of methanol reactivity on these surfaces, we have chosen O-covered

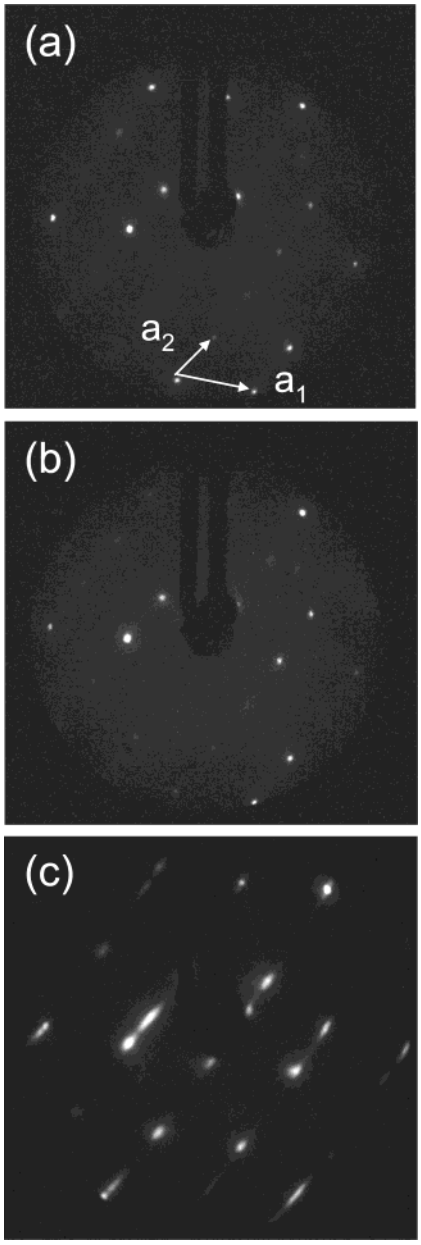

Figure 1. LEED patterns of (a) clean planar Re(12$\bar{3}$1), (b) O-covered planar Re(12$\bar{3}$1), and (c) O-induced faceted Re(12$\bar{3}$1), all taken at an incident electron beam energy of 70 eV. The O-covered planar surface is prepared by adsorption of 3 L of O_2 at 300 K, while the faceted surface is obtained by annealing the 3 L O_2-dosed surface to 900 K.

surfaces prepared with 3 L of O_2. As noted above, a fully faceted O-covered Re surface can be obtained by annealing the 3 L O_2-dosed surface to 900 K. In addition, this exposure corresponds to a near-saturation coverage of the O-covered planar surface, based on oxygen uptake studies at 300 K using AES, where the O_{KLL}/Re_{NVV} Auger peak height ratio does not increase significantly with increasing O_2 exposure beyond 3 L.[8] In a previous XPS study of oxygen adsorption at 300 K on polycrystalline Re, saturation was also observed in the O 1s signal between 3 and 5 L of O_2 exposure.[15]

The Re $4f_{7/2}$ spectrum (photoemission normal to the surface) for O-induced faceted Re(12$\bar{3}$1) is shown in Figure 3a. A minimum of four distinct features can be identified in the experimental data. Spectral decomposition into bulk and surface components places the bulk Re $4f_{7/2}$ peak at 40.3 eV, in agreement with previous measurements,[15,16] and four peaks identified with surface core level shifts (SCLS) positioned at

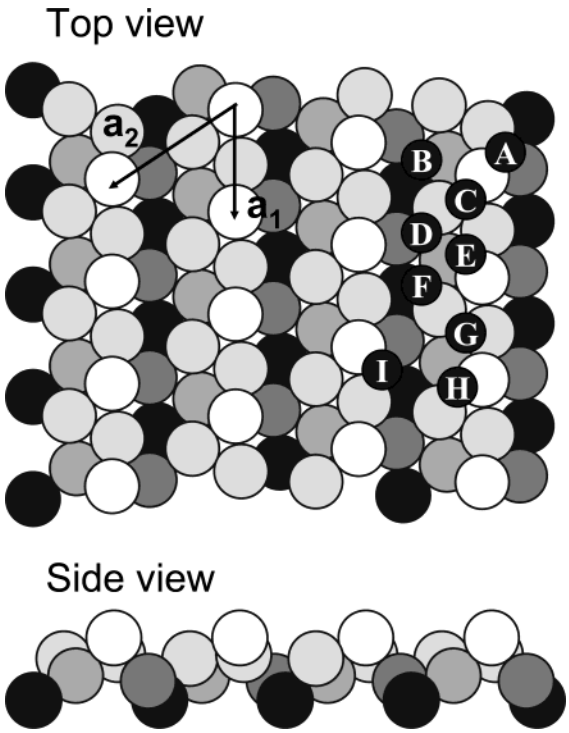

Figure 2. Hard sphere bulk-truncated model of the Re(12$\bar{3}$1) surface. The possible adsorption sites for oxygen in high-coordination hollows are labeled as A, B, C, ..., H for triply coordinated sites, and I for a hollow site coordinated with four Re surface atoms. Note that the simultaneous occupation of all labeled high-coordination sites by oxygen is unlikely due to steric hindrance.

higher binding energies than the bulk by 0.22, 0.45, 0.73, and 1.01 eV. Note that clean Re surfaces exhibit small SCLS (<0.2 eV) as determined from experimental measurements[14,16] and theoretical calculations,[17] and the peak measured for clean Re(12$\bar{3}$1) *surface* atoms (SCLS of ~0.17 eV to higher binding energy) is completely quenched upon adsorption of 3 L of O_2.[18] Hence, the shifts observed in the Re $4f_{7/2}$ spectrum for the O-induced faceted Re surface are due entirely to the presence of oxygen on the surface, and the SCLS due to Re surface atoms on clean Re(12$\bar{3}$1) does not contribute to these shifts.

The peaks at SCLS 0.22, 0.45, and 0.73 eV are assigned to surface Re atoms coordinated to one, two, and three O-adatoms, respectively, based on the correspondence of these shifts to those observed for p(2 × 1)-O on Re(0001)[16] (Table 1). The fourth surface feature with SCLS of 1.01 eV is necessary to provide an optimal fit to the Re $4f_{7/2}$ spectrum for the O-induced faceted surface and is attributed to an oxide with ReO stoichiometry.[16,19,20] The formation of ReO, characterized by a chemical shift of 1−1.1 eV to higher binding energy, has also been observed on polycrystalline Re[15,21] and Re(0001)[16] surfaces that are annealed in oxygen. On a thin-film oxide on Re(12$\bar{3}$1), formed by oxidation in 300 L of O_2 at $T \sim 1000$ K, the ReO peak grows to become the dominant feature, along with the emergence of a higher oxidation state oxide that has a comparable chemical shift (~1.7 eV) to Re_2O_3 (Figure 3a, inset and Table 1). Characterization of the thin-film oxide will be presented in detail elsewhere.[18]

The Re $4f_{7/2}$ spectrum for O-covered planar Re(12$\bar{3}$1), formed by adsorption of 3 L of O_2 at room temperature, primarily comprises a shoulder with a broad tail to higher binding energy than the bulk peak (Figure 3b). The absence of well-defined features is consistent with a disordered oxygen overlayer at 300 K, as suggested by LEED data. A good fit to the spectrum is achieved by using the same lifetime width Γ and asymmetry

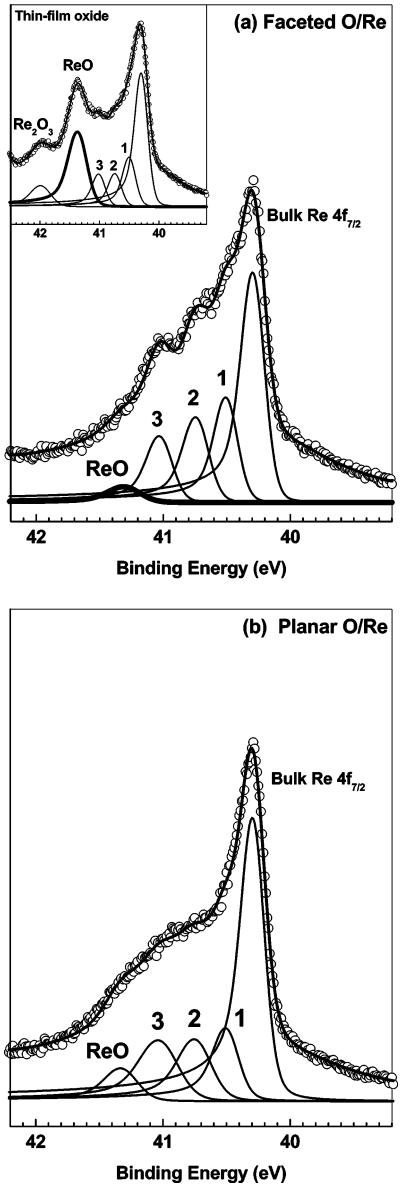

Figure 3. Doniach−Sunjic fits to the Re $4f_{7/2}$ spectra obtained for (a) an O-induced faceted Re surface, prepared by annealing a 3 L O_2-dosed surface to 900 K. Experimental data is represented by hollow circles, while fitted curves are the solid lines. The fit parameters, $\Gamma = 0.05$ eV, $\alpha = 0.16$, and Gaussian widths for bulk and surface components (1, 2, 3) are 0.18 eV, except for the ReO peak (bold line) which has a Gaussian broadening of 0.26 eV. On the thin-film oxide prepared by oxidation in 300 L of O_2 at 1000 K (inset), ReO is the majority component with some Re_2O_3 also formed. (b) O-covered planar Re surface, formed by adsorbing 3 L of O_2 at 300 K. The fit parameters, Γ, α, and Gaussian width for bulk Re $4f_{7/2}$, are the same as for the faceted surface. Gaussian broadenings for surface components 1, 2, and 3 are 0.20, 0.27, and 0.31 eV, respectively, while the width for ReO is 0.26 eV.

index α, and similar peak positions for Re−O configurations, obtained from fits to the faceted surface (Table 1). The Gaussian width for bulk Re $4f_{7/2}$ is the same as for the faceted surface (0.18 eV), while the Gaussian widths for surface features are allowed to vary, in order to account for inhomogeneity in the disordered O-overlayer. This gives Gaussian broadenings of 0.20, 0.27, and 0.31 eV for peaks due to Re coordinated with one, two, and three oxygen atoms, respectively and a Gaussian width of 0.26 eV for ReO.

3.2 Methanol Reactions over Planar and Faceted O-Modified Surfaces. The surface chemistry of methanol is studied over three surfaces: O-covered planar and faceted Re(12$\bar{3}$1) prepared with 3 L of O_2, and a thin-film oxide formed by oxidation of Re(12$\bar{3}$1) in 300 L of O_2 at 1000 K. The products detected during temperature-programmed desorption of CH_3OH adsorbed at 300 K on the *planar* O-covered Re are dihydrogen (H_2), carbon monoxide (CO), and formaldehyde (CH_2O), all evolved concomitantly in broad peaks centered at ∼410 K (Figure 4). An additional state of CO is also observed at 700 K; the two states of CO are distinguished as α-CO and β-CO for the low-temperature and high-temperature products, respectively.

TABLE 1: Surface Core Level Shifts in Re $4f_{7/2}$ for Oxygen-Modified Planar and Faceted Re(12$\bar{3}$1) Surfaces and for the Thin-Film Oxide on Re(12$\bar{3}$1)

surface	surface core level shifts (eV)				
faceted O/Re(12$\bar{3}$1)	0.22	0.45	0.73	1.01	
planar O/Re(12$\bar{3}$1)	0.21	0.45	0.73	1.03	
thin-film oxide on Re(12$\bar{3}$1)	0.20	0.44	0.71	1.06	1.68
Re(0001)-(2 × 1)-O[a]	0.21	0.42	0.70		
ReO				1.03[a]	
				1.01[b]	
Re_2O_3					1.6−1.8[c]
O-coordination[a]	1	2	3		

[a] From ref 16. [b] From ref 20. [c] From ref 15.

Hydrogen and CO production are measured by monitoring the yields of their parent molecular ions at $m/z = 2$ and $m/z = 28$, respectively. Meanwhile, formaldehyde is monitored using its major cracking fragment, CHO^+, at $m/z = 29$, instead of its molecular ion CH_2O^+ at $m/z = 30$, due to the higher abundance of the CHO^+ fragment in the mass spectral cracking pattern of formaldehyde. The production of formaldehyde is further verified by comparing the integrated peak intensity ratio of CH_2O^+ ($m/z = 30$) to CHO^+ ($m/z = 29$), which yields 0.64:1. This value is in good agreement with documented intensity ratios, ∼0.6:1, for CH_2O^+/CHO^+ cracking fragments of formaldehyde obtained in mass spectrometers.[22] No molecular CH_3OH desorption ($m/z = 32$) is observed from the O-covered *planar* surface for methanol exposures used in this study, although some desorption of the intact molecule is observed from the faceted surface, as described below. While methanol has cracking fragments that overlap with those of formaldehyde, the desorption of CH_3OH and CH_2O each gives rise to a characteristic peak temperature and line shape that is easily distinguished from the other, thus allowing for direct identification of each product. The lack of significant intensity at $m/z = 15$ and 16 indicates that measurable quantities of methyl radicals ($\cdot CH_3$) and methane (CH_4) are not formed during methanol reaction over either the planar or faceted surfaces. Also, no detectable amount of water is observed. Finally, the absence of products higher than $m/z = 32$ indicates that no C_2 and higher oxygenates, e.g., methyl formate ($HC{=}OOCH_3$) or dimethoxymethane [$CH_2(OCH_3)_2$], and no CO_2 are produced.

To determine if surface oxygen is incorporated into the products formed from methanol reaction, experiments have been performed on O-modified surfaces prepared with $^{18}O_2$. Figure 5 shows the production of CO and CH_2O from 5 L of $CH_3{}^{16}OH$ adsorbed on the ^{16}O-covered planar surface, compared with these products from the ^{18}O-labeled surface. Formaldehyde and α-CO detected during reaction on the ^{18}O-labeled surface are exclusively ^{16}O-products ($CH_2{}^{16}O$ and α-$C^{16}O$), demonstrating that these products originate directly from selective dehydrogenation of $CH_3{}^{16}OH$. In contrast, both $C^{16}O$ and $C^{18}O$ are evolved in a ratio of ∼1:2 during β-CO production, which implies that β-CO is formed via reaction with surface-bound oxygen. The incor-

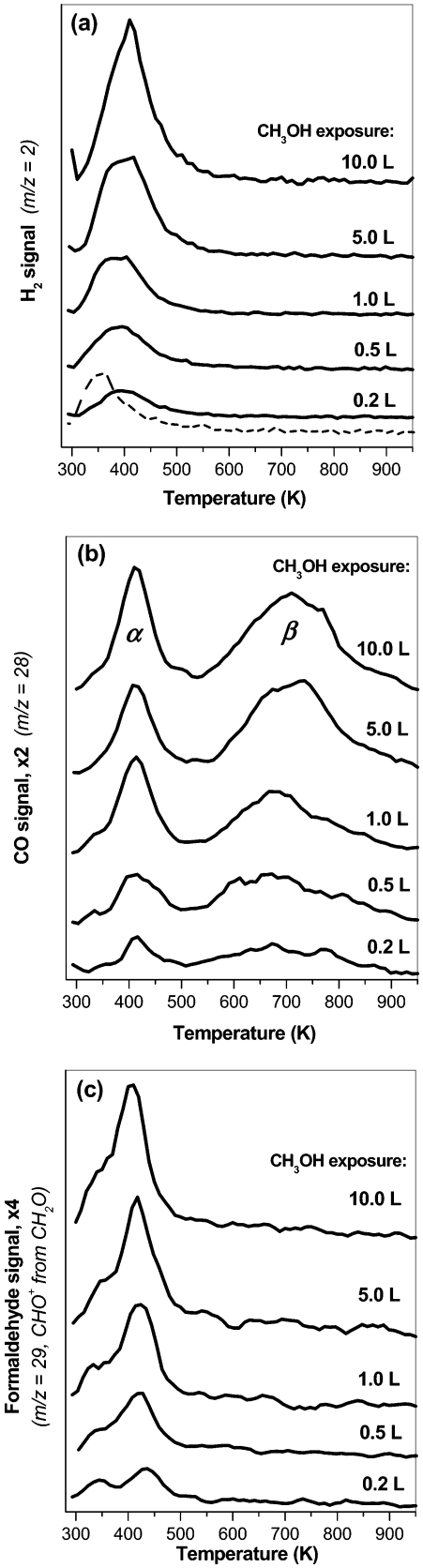

Figure 4. Temperature-programmed desorption spectra showing (a) H_2, (b) CO, and (c) CHO from CH_2O, from reaction of CH_3OH on the planar oxygen-covered Re surface. CH_3OH exposures are in Langmuirs. Hydrogen, from 15 L of H_2 exposure to the planar O-covered Re surface, gives rise to a desorption peak at ~350 K (dashed line).

poration of ^{16}O from methanol into β-CO indicates that substantial C−O bond scission in CH_3OH occurs to deposit ^{16}O to the surface. Dissociation of C−O bonds is most likely accompanied by nonselective dehydrogenation of CH_3OH; the absence of hydrocarbon (e.g., methane) production suggests that CH_x fragments are not likely to be stabilized after the C−O bonds break. Since H_2 produced from methanol reaction is evolved in a single desorption profile at ~410 K, this H_2 peak must then contain contributions from both reaction pathways of CH_3OH, i.e., nonselective decomposition and selective dehydrogenation to CH_2O and α-CO. Notably, molecular H_2 dosed on the O-covered planar Re surface gives rise to a desorption peak at 350 K (Figure 4a); hence, the production of H_2 from CH_3OH at 410 K is reaction-limited.

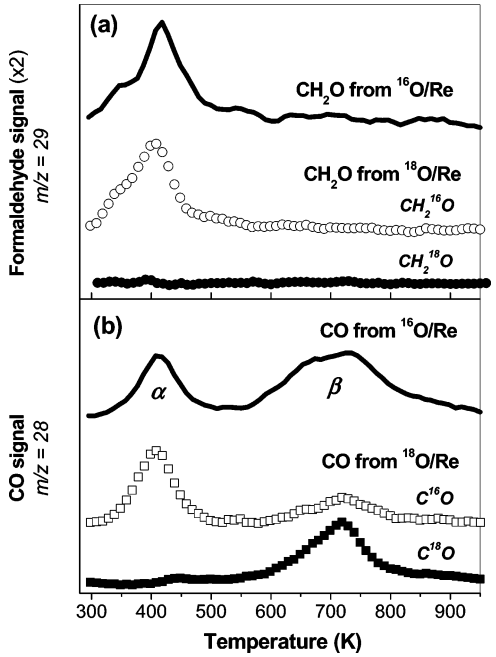

Figure 5. Temperature-programmed desorption spectra showing (a) CHO from CH_2O and (b) CO for reaction of 5 L of $CH_3{}^{16}OH$ over O-covered planar Re prepared with $^{16}O_2$ (solid line) and $^{18}O_2$ (squares and circles). Formaldehyde and α-CO are evolved exclusively as ^{16}O-products, while the majority of β-CO is formed as $C^{18}O$ from $CH_3{}^{16}$-OH reaction over the ^{18}O-labeled surface.

Product yields[23] from CH_3OH reaction on the O-covered planar surface are shown as a function of methanol exposure in Figure 6a. The yields of all products increase up to 1 L of CH_3OH exposure, at which point CH_2O and α-CO production reach plateaus. The facts that CH_2O and α-CO production saturate at the same coverage of methanol, and that both products are evolved at the same temperature, suggest that these two products are derived from a common intermediate formed upon selective dehydrogenation of CH_3OH. The saturation coverage of this intermediate achieved from adsorption of methanol at 300 K occurs at 1 L exposure. In contrast, the yields of H_2 and β-CO continue to increase for methanol exposures >1 L, indicating that nonselective CH_3OH decomposition dominates at higher methanol coverages following saturation of the selective dehydrogenation pathway.

Examination of the surface with Auger electron spectroscopy after TPD of CH_3OH to 950 K shows no residual carbon for the range of CH_3OH exposures studied. This indicates that all surface C deposited from CH_3OH nonselective decomposition has evolved as β-CO. By comparing the yield of β-CO to the total yield of products, we find that ~55% of methanol adsorbed from 5 L exposure (where α-CO and CH_2O have achieved saturation intensity) decomposes nonselectively to produce

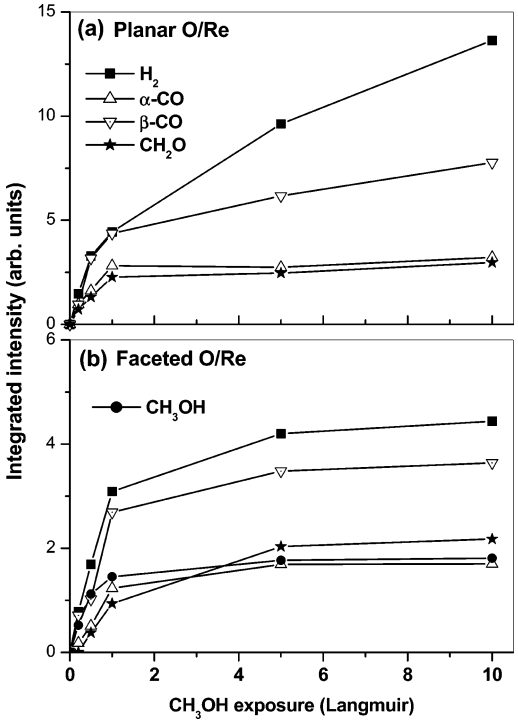

Figure 6. Integrated peak areas for products from CH_3OH reaction over O-modified (a) planar Re and (b) faceted Re, as a function of methanol exposure. Contributions from molecular CH_3OH cracking fragments that have the same *m*/*z* as reaction products from the faceted surface have been subtracted from the integrated intensities shown. Note the different scales for products from the planar and faceted surfaces.

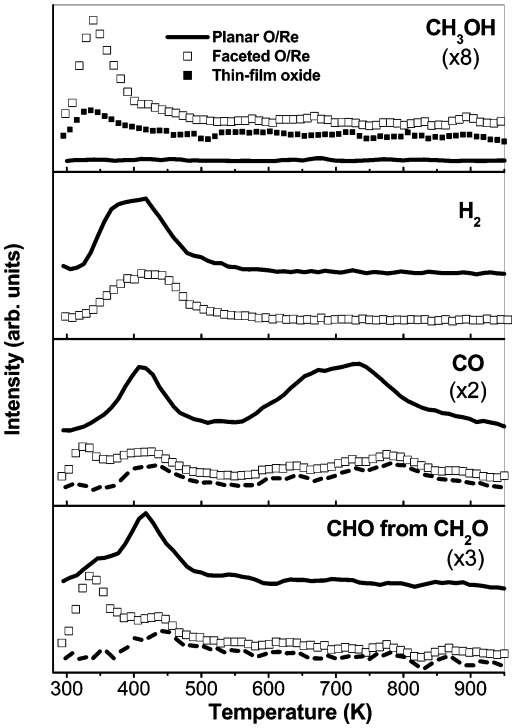

Figure 7. Temperature-programmed desorption spectra for all products evolved from 5 L of CH_3OH reaction on the O-modified planar and faceted surfaces and the thin-film oxide. Molecular CH_3OH desorbs from the faceted surface and the thin-film oxide at ~330 K. No other products are detected from the thin-film oxide. The peaks <350 K in the traces showing CO^+ and CHO^+ from the faceted surface are due to cracking fragments of CH_3OH; subtraction of molecular CH_3OH contributions from these traces shows the amount of CO and CH_2O products from the faceted surface (dashed lines).

recombinant H_2 and β-CO, with the rest of the adsorbed methanol (45%) undergoing selective reaction to form gaseous products.

The reaction of CH_3OH over the O-covered *faceted* surface yields the same products—CO, CH_2O, and H_2—at similar temperatures to those from the O-covered *planar* surface; however, the activity of the faceted surface toward methanol reaction is markedly reduced. Molecular desorption of CH_3OH ($m/z = 32$) occurs at 330 K from the faceted surface and competes with reaction, leading to a significant decrease in gaseous product formation (Figure 7). On the thin-film oxide prepared with 300 L of O_2, a small yield of molecular CH_3OH is the only desorbing species detected during TPD of 5 L of methanol (Figure 7, top panel). No reaction products of methanol are evolved from this surface. In addition, the amount of CH_3OH desorbing from the thin-film oxide is significantly less than that from the O-covered faceted surface, for the same exposure of methanol to both surfaces. Clearly, the thin-film oxide has a low activity toward methanol adsorption and is virtually inactive for reaction.

The yields of all products detected during temperature-programmed desorption of CH_3OH from the O-covered faceted surface are shown as a function of initial methanol exposure in Figure 6b. In contrast to the trend observed during methanol reaction on the planar surface, where β-CO and H_2 yields continue to increase for CH_3OH exposures >1 L, the yields of all products from methanol reaction over the faceted surface approach their plateau values at 1 L and have achieved maximum intensity by 5 L of CH_3OH exposure. This suggests that a saturation coverage of methanol is achieved by 5 L of CH_3OH exposure on the faceted surface; at this coverage, molecular CH_3OH desorption accounts for ~20% of the methanol removed during TPD. Of the remaining methanol at saturation coverage that undergoes reaction, approximately equal

TABLE 2: Yields for All C-Containing Products Evolved during Reaction of 5 L of CH_3OH over Oxygen-Modified Planar and Faceted Re(12$\bar{3}$1)[a]

	CH_3OH	α-CO	CH_2O	β-CO	total yield
planar O/Re(12$\bar{3}$1)		0.23	0.22	0.55	1
faceted O/Re(12$\bar{3}$1)	0.12	0.11	0.13	0.24	0.6

[a] Fractional yields are obtained by normalizing to the total yield of products from the planar surface.

proportions of CH_3OH follow the competing pathways of nonselective decomposition to evolve β-CO and selective dehydrogenation to produce α-CO and CH_2O. Table 2 lists the fractional yield of all C-containing products evolved during temperature-programmed desorption of 5 L of CH_3OH over the O-covered planar and faceted surfaces, normalized to the total yield of products from the planar surface. Notably, the total yield of products from the faceted surface is ~60% of that from the planar surface, which suggests that a lower saturation coverage of CH_3OH is obtained on the faceted surface than the planar surface for the same exposure of methanol at 300 K. Taken together, these results illustrate that the O-covered faceted surface is *less* facile toward CH_3OH adsorption and reaction than the O-covered planar surface.

4. Discussion

HRXPS data indicate that both the planar and faceted O-covered Re(12$\bar{3}$1) surfaces comprise surface Re atoms coordinated to various numbers of oxygen nearest neighbors, which coexist with a small concentration of oxide having ReO stoichiometry (Table 1). However, the peaks due to surface

Re−O coordination are significantly broader for the planar surface than for the faceted surface. This broadening may be attributed to disorder in the chemisorbed oxygen overlayer formed at 300 K, consistent with LEED data which shows an increase in diffuse background and the absence of long-range periodic structure for the O-covered planar surface. Oxygen is known to adsorb dissociatively on polycrystalline Re[15] and Re(0001)[16,20,24] surfaces at room temperature. On Re(0001), the oxygen monolayer forms a p(2 × 1) structure with rotational domains, with the O-adatoms located at 3-fold hollow sites.[16] On Ru(10$\bar{1}$0), another hcp substrate, oxygen occupies hollow sites that are triply coordinated with Ru atoms in both the first and second surface layers.[25] If oxygen similarly adsorbs on planar Re(12$\bar{3}$1) at hollow sites that are coordinated with three or four Re atoms, inspection of the surface reveals a number of such sites available for oxygen occupation (Figure 2). It appears that the multiplicity of Re surface sites, giving rise to a range of inequivalent Re−O bond lengths, is the origin of the observed broadening in the Re $4f_{7/2}$ spectrum for O-covered planar Re. Adsorption of oxygen at room temperature on polycrystalline Re, where a distribution of oxygen adsorption sites is expected, also forms an inhomogeneous oxygen overlayer as reflected in broadening of measured Re 4f peaks.[15,21]

The formation of ReO on Re(12$\bar{3}$1) upon oxygen adsorption at 300 K is consistent with previous studies: ReO readily forms on polycrystalline Re following exposure to O_2 at room temperature[15,20] but not on Re(0001).[16] Likewise, we expect atomically rough Re(12$\bar{3}$1), with six layers of exposed surface atoms, to be more facile toward oxide formation than close-packed Re(0001). This is evident from the different oxidation states of Re oxides formed upon high-temperature oxidation of Re(0001), compared with Re(12$\bar{3}$1). When Re(0001) is oxidized with 300 L of O_2 at $T \sim 1000$ K, the resulting surface oxide has a maximum oxidation state of Re^{2+}, while oxidation of Re(12$\bar{3}$1) using similar conditions produces a thin-film oxide comprising both ReO and Re_2O_3. While Re is known to form a variety of stable bulk oxides (ReO_2, ReO_3, Re_2O_7), previous XPS studies have established chemical shifts between 2.5 and 6 eV for Re in oxidation states ranging from Re^{4+} to Re^{7+}.[26,27] The fact that no chemical shift >1.7 eV is observed confirms that no oxide with an oxidation state higher than Re^{3+} is formed on any of the O-modified Re surfaces studied herein.

The reaction pathways of methanol over the *planar* and *faceted* oxygen-modified Re surfaces are qualitatively similar, despite quantitative differences in their product yields. The proposed reaction scheme for methanol on both surfaces is described below.

Nonselective decomposition competes with selective dehydrogenation of CH_3OH over the O-modified Re surfaces. The presence of both $C^{18}O$ and $C^{16}O$ formed by atom recombination during $CH_3{}^{16}OH$ reaction over the ^{18}O-labeled surface, coupled with H_2 evolution with a peak at 410 K, indicates that nonselective decomposition of methanol occurs around this temperature. In conjunction, some of the adsorbed methanol may undergo O−H bond scission to form surface methoxy:

$$CH_3OH \rightarrow CH_3O(a) + H(a) \quad (1)$$

Subsequently, methoxy may partially dehydrogenate to transient formaldehyde, some of which desorbs, giving rise to the CH_2O peak observed during TPD.

$$CH_3O(a) \rightarrow CH_2O(a) + H(a) \quad (2)$$

$$CH_2O(a) \rightarrow CH_2O(g) \quad (3)$$

In competition, formaldehyde from partial dehydrogenation of methoxy may also undergo rapid elimination to CO, i.e., α-CO at ∼410 K.

$$CH_3O(a) \rightarrow CH_2O(a) + H(a) \rightarrow CO(g) + 3H(a) \quad (4)$$

Once formed, H(a) from reactions 1, 2, and 4 desorbs rapidly as H_2(g), contributing to the hydrogen peak observed during TPD. Since molecular H_2 dosed on the O-modified Re surfaces desorbs at ∼350 K (Figure 4a), the production of H_2 from CH_3OH at 410 K is concluded to be limited by dehydrogenation pathways of methoxy.

Although direct identification of surface methoxy is not obtained, the absence of surface ^{18}O incorporation into CH_2O and α-CO formed during $CH_3{}^{16}OH$ reaction on the isotopically labeled surface, and the concomitant evolution of H_2 with these oxygenates, strongly indicate that CH_2O and α-CO both originate from a dehydrogenation pathway of methanol. The correspondence in peak temperatures and profiles for CH_2O and α-CO provides further evidence for a common intermediate to both products. All this is consistent with a methoxy precursor to CH_2O and α-CO. Indeed, numerous studies on methanol reactions over clean metal,[28,29] O-covered metal,[30−32] and oxide[1,33,34] surfaces identify methoxy as the primary intermediate to formaldehyde. The possibility that a formate (HCOO) intermediate may also be formed is discounted. While oxidation of methoxy to surface formate occurs readily on oxide[35] and O-modified metal[36] surfaces, the decomposition of HCOO generally proceeds via dehydrogenation to form CO_2 and H_2 and/or dehydration to CO and H_2O.[37,38] The absence of CO_2 and H_2O accompanying CO production during methanol TPD suggests that surface formate is not likely formed on the O-modified Re surfaces.

The rapid dehydrogenation of methoxy to CO is precedented in methanol reactions over transition metal surfaces[9,39] and is proposed to occur via a transient formaldehyde intermediate.[40] When these surfaces are modified with oxygen, formaldehyde (from partial dehydrogenation of methoxy) is stabilized on the surface, and its subsequent decomposition to CO is partially inhibited, giving rise to the evolution of gaseous CH_2O together with some CO.[41] We propose that similar competing pathways occur during methanol reaction on the oxygen-modified Re surfaces, based on the evolution of CH_2O coincident with CO during methanol TPD. Spectroscopic confirmation for the possible formation of methoxy and formaldehyde intermediates during CH_3OH reaction on the O-modified Re surfaces will be the subject of future study.

Remarkable differences in activity toward methanol reaction are observed between the thin-film oxide and the O-modified planar and faceted Re surfaces. Methanol does not undergo reaction on the thin-film oxide, in contrast to the planar and faceted surfaces where products due to nonselective decomposition and dehydrogenation pathways are evolved. We attribute the lack of activity of the thin-film oxide to the high concentration of Re oxides, mainly ReO and some Re_2O_3, that are present on this surface. This is consistent with the study of Bowker et al.,[10] which reported that an oxide with ReO stoichiometry formed on polycrystalline Re is inert toward methanol. These results indicate that low oxidation state oxides (ReO and possibly Re_2O_3) passivate Re-based surfaces toward methanol adsorption and reaction, thereby demonstrating that Re^{2+} and Re^{3+} are not likely to be the catalytically active species for methanol oxidation.

Methanol reactivity over the O-modified planar and faceted Re surfaces is also markedly different. The saturation coverage

of methanol on the faceted surface is significantly less than that on the planar surface, for the same exposure of methanol to both surfaces (Table 2). In addition, some methanol desorbs without reacting on the faceted surface, while all of the adsorbed methanol on the planar surface undergoes reaction or decomposition: clearly, the O-modified faceted surface is less reactive toward methanol. The fact that ReO is present in comparable amounts on both surfaces suggests that catalytically inactive Re^{2+} alone cannot account for the different activities of these two structurally distinct surfaces. The reduced activity of the faceted surface may be due, in part, to the introduction of nanometer scale facets of more closely packed $(11\bar{2}1)$ and $(01\bar{1}0)$ facet planes, compared to the open coordination of the planar O-covered Re$(12\bar{3}1)$ surface. Differences in methanol reactivity have also been observed over TiO_2,[42] CeO_2,[43] ZnO,[44] and SnO_2[45] thin films and single crystals with different morphologies and crystallographic orientations. Rutile $TiO_2(001)$ exposing {114} facets is more active toward methanol oxidation than the {011}-faceted (001) surface,[42] and rutile TiO_2 powders also exhibit higher methanol adsorption activity than the anatase polymorph.[46] Similarly, strikingly different activities for methanol adsorption and reaction are observed over $CeO_2(111)$ and (100), with the (100) surface being significantly more reactive.[43] Likewise, ZnO in the $(000\bar{1})$-O polar face is inactive toward methanol, while both dehydrogenation and oxidation reactions occur on the (0001)-Zn polar face.[44] SnO_2 films in the (110) phase also demonstrate higher activity for methanol dissociation and oxidation in comparison with films comprising (211) and (301) phases.[45] Taken together with our findings on planar and faceted O-modified Re, all these studies demonstrate that changes in local geometric structure can significantly affect the activity of model oxidation catalysts toward methanol reaction.

The inhomogeneous distribution of oxygen on the O-covered planar surface may also play a role in its increased activity toward methanol reaction. Methanol conversion to methoxy is known to occur primarily at open high-coordination sites (i.e., oxygen vacancies) on oxide and oxidized metal surfaces.[47,48] The planar Re$(12\bar{3}1)$ surface presents a number of inequivalent triply coordinated sites for oxygen adsorption (Figure 2); however, the absence of an ordered oxygen superstructure on the planar surface suggests that there is no strong driving force for oxygen occupation at one preferred site over another. Thus, it is quite likely that vacancies are present at high-coordination sites on the O-covered planar surface, which may promote CH_3OH reaction. In contrast, significant amounts of oxygen vacancies are not expected on the faceted surface as a thermally annealed chemisorbed oxygen overlayer is necessary to stabilize the facet planes. (The faceted Re surface reverts to a planar morphology following partial loss of oxygen from the surface.[18] Furthermore, the more closely packed $(11\bar{2}1)$ and $(01\bar{1}0)$ facet planes of the faceted surface have lower densities of high-coordination sites present for methoxy coordination, as compared with the planar $(12\bar{3}1)$ surface. Scanning tunneling microscopy (STM) studies on the O-modified Re surfaces are planned in order to elucidate the possible role of oxygen vacancies on the different activities exhibited by these surfaces.

The different morphologies of the O-modified planar and faceted Re surfaces do not appear to play a significant role in the selectivity of methanol reaction products. Notably, of the methanol that undergoes reaction on the faceted surface, the branching ratio toward dehydrogenation products (CH_2O and CO), versus products from complete decomposition, is very similar to that from the planar surface (Table 2). This is a surprising result since methanol reaction pathways on several other metal (Pt,[9] Pd[49]) and oxide (TiO_2,[42] ZrO_2[50]) surfaces are reported to be sensitive to geometrical structure. Specifically, on well-defined Pd crystallites comprising (111) and (100) facets, methoxy dehydrogenation to CO is favored on facet planes, while C−O bond scission in methoxy occurs on edge sites at the boundaries of facet planes.[49] Similarly, we might expect that Re edge atoms between the $(11\bar{2}1)$ and $(01\bar{1}0)$ facets, with a lower coordination than atoms within the facet planes, would be more aggressive toward CH_3OH reaction/decomposition. The fact that this is not observed suggests that these edge sites may be blocked when the faceted surface forms. One possible scenario is that ReO moieties on the faceted surface decorate the facet edges, thus effectively suppressing the activity of these edge sites toward methanol. Structural investigations using STM are necessary to test this hypothesis.

The formation of methanol partial oxidation products, CH_2O and α-CO, from the O-modified Re$(12\bar{3}1)$ surfaces suggests that they are promising model substrates for studying the catalytic oxidation of methanol to methylal. The fact that gaseous CH_2O is evolved indicates that transient surface-bound CH_2O_{ads} species may be formed before undergoing dehydrogenation or desorption channels. No oxidation of CH_2O_{ads} to formate (HCOO) or dioxymethylene $(H_2COO)^{2-}$—a precursor to methylal—is observed, based on the distribution of products that can be attributed entirely to methoxy. We propose that the absence of dioxymethylene is due to the low oxidation state of our O-modified Re surfaces, since dioxymethylene is known to form via reaction of surface-bound CH_2O with *lattice* oxygen in Re oxide catalysts.[5] Under catalytic conditions, methanol from the reaction feed stream will replenish that consumed in dioxymethylene formation, leading to the coexistence of dioxymethylene and methoxy species on the catalyst surface that will react to yield methylal. On this basis, sequential adsorption studies of methanol onto a CH_3OH-precovered ReO_x surface having bulk oxide stoichiometry (with the preadsorbed CH_3OH in various stages of decomposition) may help elucidate the mechanistic details of methanol conversion to methylal.

5. Conclusions

Methanol reacts via competing pathways of nonselective decomposition to H_2 and recombinant CO and selective O−H scission to methoxy on the O-covered planar and faceted Re surfaces. Methoxy also decomposes through two competing pathways: partial dehydrogenation to evolve gaseous CH_2O and rapid H-elimination to CO(g). The branching ratios for methanol toward CH_2O, CO, and products due to nonselective decomposition are similar over the planar and faceted surfaces, which suggest that differences in geometrical structure do not affect the selectivity of methanol reaction products. However, the activity for methanol reaction over the O-modified Re surfaces *decreases* in the following order: planar O/Re > faceted O/Re > thin-film oxide/Re, with the thin-film oxide exhibiting no activity toward methanol reaction. The low activity of the thin-film oxide is attributed to the formation of low oxidation state oxides (ReO, Re_2O_3). Methanol reactivity over the planar and faceted O-covered surfaces differs in two distinct ways: (1) all of the adsorbed methanol on the planar surface undergoes reaction, while some molecular CH_3OH desorption occurs from the faceted surface and (2) methanol reaction over the faceted surface leads to an overall decrease in product yield compared to the planar surface, even after accounting for the fraction of CH_3OH that desorbs molecularly. The enhanced activity of the planar surface may be due to the probable presence of O-vacancies, and to differences in local geometric structure, as compared to the faceted surface.

Acknowledgment. This work has been supported in part by the U.S. Department of Energy, Office of Basic Energy Sciences, and by the Army Research Office. The research is carried out in part at the National Synchrotron Light Source, Brookhaven National Laboratory, which is supported by the U.S. Department of Energy, Division of Materials Sciences and Division of Chemical Sciences, under Contract No. DE-AC02-98CH10886. A.C. thanks Dr. Gunther K. Wertheim for helpful discussions concerning the fitting of HRXPS data.

References and Notes

(1) Busca, G. *Catal. Today* **1996**, *27*, 457.
(2) Cheng, W.-H. *Acc. Chem. Res.* **1999**, *32*, 685.
(3) Ai, M. *J. Catal.* **1978**, *54*, 426.
(4) Forzatti, P.; Tronconi, E.; Busca, G.; Tittarelli, P. *Catal. Today* **1987**, *1*, 209.
(5) Yuan, Y.; Iwasawa, Y. *J. Phys. Chem. B* **2002**, *106*, 4441.
(6) Yuan, Y.; Shido, T.; Iwasawa, Y. *Chem. Commun.* **2000**, 1421.
(7) Yang, T. J.; Lunsford, J. H. *J. Catal.* **1987**, *103*, 55.
(8) Wang, H.; Chen, W.; Chan, A. S. Y.; Madey, T. E. To be published.
(9) Wang, J.; Masel, R. I. *J. Vac. Sci. Technol. A* **1991**, *9*, 1879.
(10) Francis, S. M.; Corneille, J.; Goodman, D. W.; Bowker, M. *Surf. Sci.* **1996**, *364*, 30.
(11) Thiry, P.; Bennett, P. A.; Kevan, S. D.; Royer, W. A.; Chaban, E. E.; Rowe, J. E.; Smith, N. V. *Nucl. Instrum. Methods Phys. Res. Sect. A* **1984**, *222*, 85.
(12) Pelhos, K.; Abdelrehim, I. M.; Nien, C.-H.; Madey, T. E. *J. Phys. Chem. B* **2001**, *105*, 3708.
(13) Doniach, S.; Sunjic, M. *J. Phys. C* **1970**, *3*, 185.
(14) (a) Martensson, N.; Saalfeld, H. B.; Kuhlenbeck, H.; Neumann, M. *Phys. Rev. B* **1989**, *39*, 8181. (b) Also communications with Gunther K. Wertheim, who developed the fitting model to account for the Re $5p_{1/2}$ contribution into the Re 4f spectra.
(15) Morant, C.; Galan, L.; Sanz, J. M. *Anal. Chim. Acta* **1994**, *297*, 179.
(16) Ducros, R.; Fusy, J. *J. Electron Spectrosc. Relat. Phenom.* **1987**, *42*, 305
(17) Ruban, A. V.; Skriver, H. L.; Norskov, J. K. *Phys. Rev. B* **1999**, *59*, 15990.
(18) Chan, A. S. Y.; Wang, H.; Ulrich, M. D.; Rowe, J. E.; Madey, T. E. To be published.
(19) Weber, B.; Cassuto, A. *Surf. Sci.* **1973**, *36*, 81.
(20) Ducros, R.; Alnot, M.; Ehrhardt, J. J.; Housley, M.; Piquard, G.; Cassuto, A. *Surf. Sci.* **1980**, *94*, 154.
(21) Liu, P.; Shuh, D. K. *J. Electron Spectrosc. Relat. Phenom.* **2001**, *114*, 319.
(22) (a) NIST Mass Spectrometry Data Center. http://webbook.nist.gov. (b) *Eight Peak Index of Mass Spectra*, 3rd ed.; The Royal Society of Chemistry: U.K., 1983.
(23) Product yield is quantified by summation of the integrated peak intensities of all major cracking fragments attributed to each product, ignoring small differences (∼10%) in the relative ionization sensitivities for CO, CH_2O, and CH_3OH. See, for example, Flaim, T. A.; Ownby, P. D. *J. Vac. Sci. Technol.* **1971**, *8*, 661.
(24) Tatarenko, S.; Dolle, P.; Morancho, R.; Alnot, M.; Ehrhardt, J. J.; Ducros, R. *Surf. Sci.* **1983**, *134*, L505.
(25) Baraldi, A.; Lizzit, S.; Paolucci, G. *Surf. Sci.* **2000**, *457*, L354.
(26) Seah, M. P.; Dench, W. A. *Surf. Interface Anal.* **1979**, *1*, 2.
(27) Cimino, A.; de Angelis, B. A.; Gazzoli, D.; Valigi, M. *Z. Anorg. Allg. Chem.* **1980**, *460*, 86.
(28) Chen, A. K.; Masel, R. *Surf. Sci.* **1995**, *343*, 17.
(29) Barros, R. B.; Garcia, A. R.; Ilharco, L. M. *J. Phys. Chem. B* **2001**, *105*, 11186.
(30) Queeney, K. T.; Friend, C. M. *J. Chem. Phys.* **1998**, *109*, 6067.
(31) Francis, S. M.; Leibsle, F. M.; Haq, S.; Xiang, N.; Bowker, M. *Surf. Sci.* **1994**, *315*, 284.
(32) de Barros, R. B.; Garcia, A. R.; Ilharco, L. M. *Surf. Sci.* **2002**, *502*, 156.
(33) Wong, G. S.; Kragten, D. D.; Vohs, J. M. *J. Phys. Chem. B* **2001**, *105*, 1366.
(34) Wang, Q. G.; Madix, R. J. *Surf. Sci.* **2002**, *496*, 51.
(35) Edwards, J. F.; Schrader, G. L. *J. Phys. Chem.* **1985**, *89*, 782.
(36) Mudalige, K.; Trenary, M. *Surf. Sci.* **2002**, *504*, 208.
(37) Grant, A. W.; Larsen, J. H.; Perez, C. A.; Lehto, S.; Schmal, M.; Campbell, C. T. *J. Phys. Chem. B* **2001**, *105*, 9273.
(38) Houtman, C.; Barteau, M. A. *Surf. Sci.* **1991**, *248*, 57.
(39) Akhter, S.; White, J. M. *Surf. Sci.* **1986**, *167*, 101.
(40) Davis, J. L.; Barteau, M. A. *Surf. Sci.* **1988**, *197*, 123.
(41) Wang, J.; DeAngelis, M. A.; Zaikos, D.; Setiadi, M.; Masel, R. I. *Surf. Sci.* **1994**, *318*, 307.
(42) Kim, K. S.; Barteau, M. A. *Surf. Sci.* **1989**, *223*, 13.
(43) Ferrizz, R. M.; Wong, G. S.; Egami, T.; Vohs, J. M. *Langmuir* **2001**, *17*, 2464.
(44) Vohs, J. M.; Barteau, M. A. *Surf. Sci.* **1986**, *176*, 91.
(45) Kawabe, T.; Tabata, K.; Suzuki, E.; Nagasawa, Y. *Surf. Sci.* **2001**, *482*−*485*, 183.
(46) Lusvardi, V. S.; Barteau, M. A.; Farneth, W. E. *J. Catal.* **1995**, *153*, 41.
(47) Queeney, K. T.; Friend, C. M. *J. Phys. Chem. B* **1998**, *102*, 5178.
(48) Gercher, V. A.; Cox, D. F.; Themlin, J. M. *Surf. Sci.* **1994**, *306*, 279.
(49) Schauermann, S.; Hoffman, J.; Johanek, V.; Hartmann, J.; Libuda, J.; Freund, H.-J. *Angew. Chem. Int. Ed.* **2002**, *41*, 2532.
(50) Dilara, P. A.; Vohs, J. M. *Surf. Sci.* **1994**, *321*, 8.